Excitons in CdTe quantum wires with strain-induced lateral confinement

D. Brinkmann, G. Fishman, C. Gourgon, Le Si Dang, A. Löffler, and H. Mariette
Laboratoire de Spectrométrie Physique, Université Joseph Fourier Grenoble 1, France
Equipe CEA–CNRS ''Microstructures de Semiconducteurs II-VI,'' Boîte Postale 87, 38402 Saint Martin d'Hères Cedex, France
(Received 28 December 1995; revised manuscript received 4 March 1996)

Using a two-step epitaxial growth process we have fabricated nanometer-scale quantum wires through the modulation of the in-plane lattice constant of a [110] CdTe/$Cd_xZn_{1-x}Te$ quantum well grown on top of a [001] CdTe/$Cd_xZn_{1-x}Te$ strained superlattice. With respect to the unmodulated [110] quantum well, the photoluminescence of these quantum wires presents a large redshift which depends strongly on the excitation density. The results compare very well with a theoretical model assuming no strain relaxation in the structure. In this framework, we show that (i) the hole is confined via the Coulomb attraction of the electron and not via the valence-band offset, and (ii) due to the nonlinearity of the piezoelectric coefficient in CdTe, a lateral piezoelectric field is present in these strained modulated [110] wires. [S0163-1829(96)04627-9]

Among all the one-dimensional (1D) semiconductors (SC's) which have been fabricated in recent years,[1–4] the one obtained by strain-induced lateral confinement (called S1D below) (Refs. 5–7) is the most controversial. More precisely the photoluminescence (PL) experiments, which are a very powerful tool for studying two-dimensional (2D) SC's or quantum wells (QW's) as well as quantum well wires (QWW's), have given rise to a controversy not only as to the origin of the PL lines but even as to the existence itself of a S1D.[8,9] The problem is the following: on one side the PL data, which are reported only for the $In_xGa_{1-x}As/GaAs$ strained system, are understood as resulting from the *S*1D;[5,9] on the other side, the calculation performed within elastic theory framework results in a full relaxation of the lattice, so that the strain modulation that is supposed to create confinement in the second direction, i.e., to create the wire, does not exist.[8] In this last case the origin of the PL lines is of course unexplained. The aim of this paper is to bring about additional information about this problem: we observe the PL emission of *S*1D made with another strained system, namely CdTe/$Cd_xZn_{1-x}Te$, and we show the existence of a lateral piezoelectric field present in this 1D structure.

In order to obtain these results, for the II-VI materials we have developed a molecular-beam epitaxy (MBE) growth technique called cleaved edge overgrowth initiated by Pfeiffer *et al.*[10] for the III-V's. This has allowed us to obtain PL spectra for CdTe *S*1D. To account for the results of optical measurements, we have assumed (as in Ref. 5) that there is no lattice relaxation in the *S*1D structure. We have then calculated (i) the confinement energies of both electrons and holes, (ii) the energy-dispersion curves of the conduction and valence bands, and (iii) the exciton binding energies. We then obtained that the exciton transition energies are in good agreement with the experiments. Moreover the dependence on the excitation density of QWW transition energies is also explained by taking into account the nonlinear piezoelectric effect specific to CdTe.[11]

The strain modulation is produced by a first epitaxial step, namely the MBE growth of a [001] CdTe/$Cd_{0.77}Zn_{0.23}Te$ strained superlattice (SSL) pseudomorph to a $Cd_{0.88}Zn_{0.12}Te$ substrate. To insure pseudomorphic growth whatever the total thickness of the SSL, we design the SSL in order to have an average strain close to zero.[12] It contains 100 periods of CdTe (10 nm) and $Cd_{0.76}Zn_{0.24}Te$ (10 nm). The second step MBE growth on the [110] cleaved face (see the upper part of Fig. 1) consists of deposing a sequence of $Cd_{0.92}Zn_{0.08}Te$ (20 nm), CdTe (10 nm), and $Cd_{0.92}Zn_{0.08}Te$ (40 nm). Therefore the band gap of the 10-nm [110]-CdTe/$Cd_xZn_{1-x}Te$ QW is spatially modulated by strains in regions grown above the [001]-CdTe/$Cd_xZn_{1-x}Te$ SSL providing a lateral confinement to carriers and forming QWW's. PL measurements were carried out at 1.8 K with a mapping setup having a spatial resolution of 15 μm (laser spot size), which allows one to select precisely any place on the sample. The sample was excited with an Ar^+ laser with power density ranging from 5 W/cm^2 to more than 1 kW/cm^2. Typical PL spectra of the structure are presented in Fig. 1. These PL spectra are obtained from three different regions of the sample, as indicated in the upper part of the figure. The PL of the SSL and of the [110] QW exhibits two lines which can be attributed to recombination of intrinsic heavy-hole excitons (e_1h_1) and of excitons bound to residual impurities (lines *C* and *Y*).[13,14] The PL of QWW's at low excitation is a broadband shifted by about 40 meV to the red relative to the [110] QW emission, in agreement with estimates of carrier localization by strain modulation in this structure as demonstrated below. Note that due to the laser spot size (15 μm) compared to the wire region one (1 μm), we expect to observe, when exciting into this region [spectrum (*c*) in Fig. 1], two contributions due to both the QWW and the [110] QW; since the PL of the QWW's dominates over that of the [110] QW, the localization in the wires is quite efficient. To ascertain the origin of the broad PL line as due to the QWW emission, we record the PL intensity at various wavelengths along the cleaved edge sample. From these profile measurements, shown in Fig. 2, it is clear that the emission of the broadband at 1.578 eV comes only from the part of the [110] QW grown over the SSL, in contrast to the substrate and the [110] QW emissions, which are present all over the cleaved edge.

Another characteristic feature of the QWW emission is its strong dependence on the excitation density, as illustrated on Fig. 3. The emission coming from the QWW appears at 40

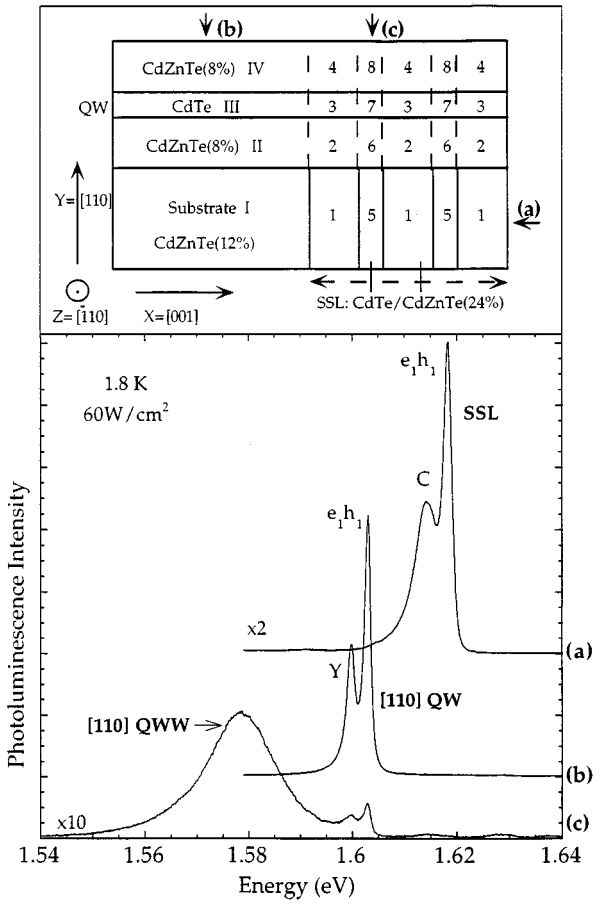

FIG. 1. PL spectra of the sample obtained by overgrowth of a [110] $CdTe/Cd_xZn_{1-x}Te$ QW on a [001] $CdTe/Cd_xZn_{1-x}Te$ strained superlattice. Spectra are obtained from three different regions on the sample, as indicated in the upper part: (a) PL of [001] strained superlattice; (b) PL of 2D [110] QW grown above the substrate; (c) PL of [110] quantum-well wires grown above the superlattice. The scheme represents also a side view of the sample with the notations used for all the domains present in this structure.

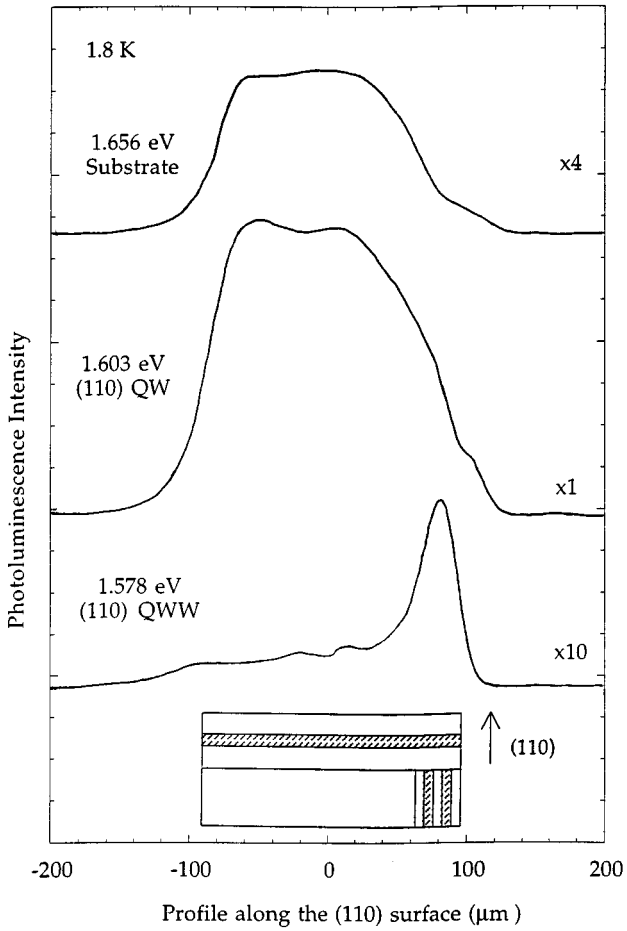

FIG. 2. Luminescence profiles vs the position on the cleaved [110] surface at three different wavelengths corresponding, respectively, to the substrate, the [110] quantum well, and the [110] quantum-well wires.

meV below that from the [110] QW for the lowest excitation density, and is blueshifted by almost 30 meV when the power density is larger than 1 kW/cm^2. This behavior suggests both the presence of an electrical field in the [110]-modulated QW and the screening of this field when the power density is increased. Such an electrical field (and its fluctuations) could be at the origin of the photoluminescence linewidth obtained for the QWW emission. Then we would expect that the screening of this field will lead to a decrease of the broadening.[15] That is not the case for the high excitation densities (see Fig. 3), which suggests the importance of many-body effects.

We now come to the theoretical part of this paper. The first step of the calculation is to evaluate the strain in the different parts of the structure by solving Hook's tensorial equations. In order to do that, we assume that there is no relaxation of any kind (neither plastic nor elastic) in the sample. This hypothesis means that the strain modulation produced by the SSL is entirely transferred to the [110] QW, which should be an overestimation of strain according to authors who have used continuum elasticity theory.[8] However such an assumption is well supported by our experimental data, which show that the electronic properties of a [110] QW are strongly affected by the presence of strained layers 200 Å below. In the following, we refer to the axis system: $X=[001]$, $Y=[110]$, and $Z=[\bar{1}10]$. To calculate the deformations in the various parts of the sample (domains 2, 3, and 4, and 6, 7, and 8 in the upper part of Fig. 1), we consider that the QWW's are coherently grown on both the SSL (domains 1 and 5) and the uniformly strained [110] QW (domains II, III, and IV). In other words, it is assumed that in QWW domains, deformations along the X direction are imposed by the SSL, those along the Y direction are imposed by the [110] QW, and those along the Z direction are common to both the [110] QW and SSL. It is then possible to calculate the confinement potential in the different parts of the structure, and the result for electrons is displayed in Fig. 4. This potential profile has been calculated taking into account successively the chemical band offset, the contribution of the strain, and the lateral piezoelectric effect present in the QWW's. We want to point out that in an ideal [110] QW, for which the polarization **P** is parallel to the QW plane, the polarization cannot create any piezoelectric charges.[16] It is also important to note that, in our case, this lateral piezoelectric field does not arise from interface fluctuations as recently reported for [110]-strained QW's,[16] but from the nonlinear

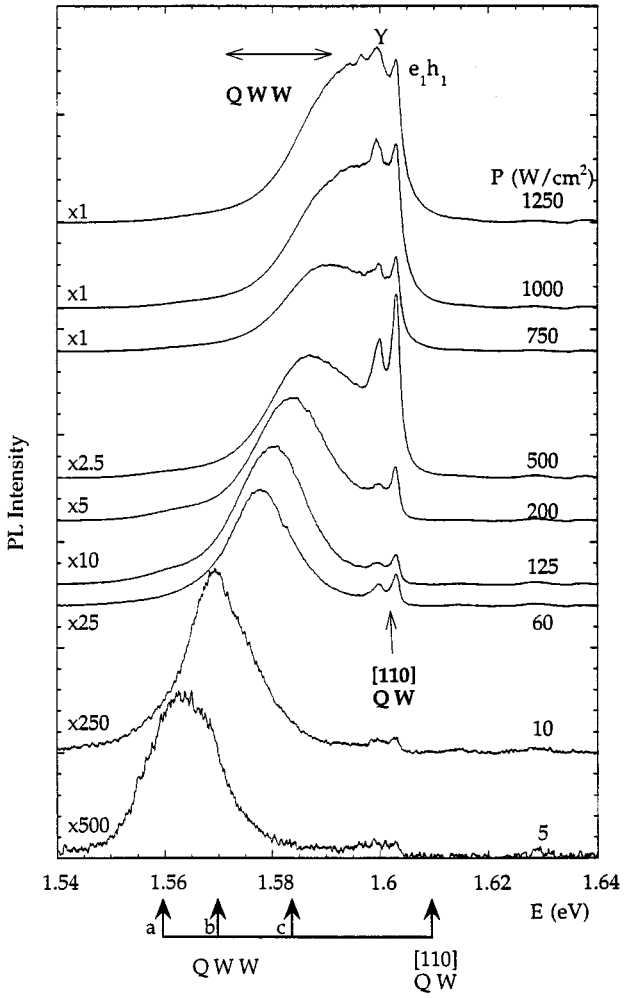

FIG. 3. PL spectra of the 2D [110] QW and the [110] QWW's obtained at low temperature for various excitation densities. The exciton recombination in the QWW is shifted to the high energy by 25 meV, in contrast to the exciton lines e_1h_1 and Y in the [110] QW. The arrows give the calculated energy transitions for the excitonic one in the [110] QW, for the excitonic one in the [110] QWW taking into account (a) or not (b) the lateral piezoelectric field, and for the electron-hole one (c) in these [110] QWW's.

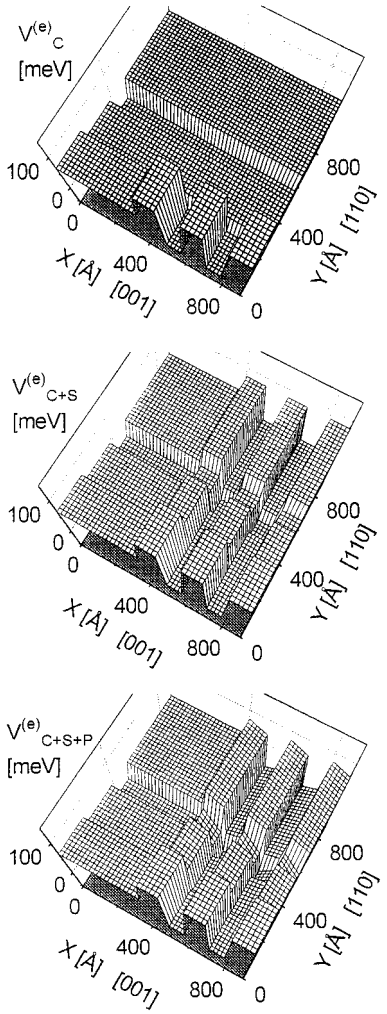

FIG. 4. Confinement potential for the electrons along the X[001] direction corresponding to the growth axis of the strained superlattice, and the Y[110] one corresponding to the growth direction of the overgrown quantum well. $V_C^{(e)}$ represents the potential taking into account only the chemical band offset (100% in the conduction band), $V_{C+S}^{(e)}$ the potential obtained by adding the contribution of the strains, and $V_{C+S+P}^{(e)}$ the potential obtained by including also the lateral piezoelectric field present in such a modulated [110] structure.

piezoelectric effect present in CdTe,[11] as we will show below. For the holes we have taken into account the contribution of the strain via the Bir-Pikus Hamiltonian and the lateral piezoelectric effect. Incidentally we can note that it is not possible to represent the hole potential on a figure, as is done for the electrons in Fig. 4: this simply results from the fact that the Bir-Pikus Hamiltonian is a nondiagonal matrix and not a scalar, as is the case for the electron. This is similar to the case of QW grown along the [112] direction, for which it is not possible to define a quantum-well depth for the holes.[17]

The piezoelectric polarization in our [110] structure (see the inset of Fig. 1) is directed along the X direction, and is given by

$$\mathbf{P}_{[110]}=[e_{14}(\varepsilon_{YY}-\varepsilon_{ZZ}),0,0], \tag{1}$$

where ε_{YY} and ε_{ZZ} are deformations along the Y and Z directions, respectively. In our pseudomorphic growth model ε_{YY} as well as ε_{ZZ} are the same in domains 3 and 7, so that there should be no induced electric field in these domains. However, the deformation ε_{XX} along the X direction is modulated by the SSL. This will result in a modulation of the volume of CdTe, and consequently a modulation of the piezoelectric field coefficient e_{14} due to the piezoelectric nonlinearity in this material.[11] This modulation amounts to about $\Delta e_{14}=0.06$ C/m^2, which produces an electric field **E**. To calculate **E**, we assume that the potential difference created by the piezoelectric effect is compensated for over one SSL period, i.e., **E** is proportional to the polarization difference in domains 2 and 6 (3 and 7, respectively): the deduced value of **E** is then 4×10^4 V/cm.

Electron and hole wave functions were calculated using the method described in Refs. 17–19. In the 2D [110] QW,

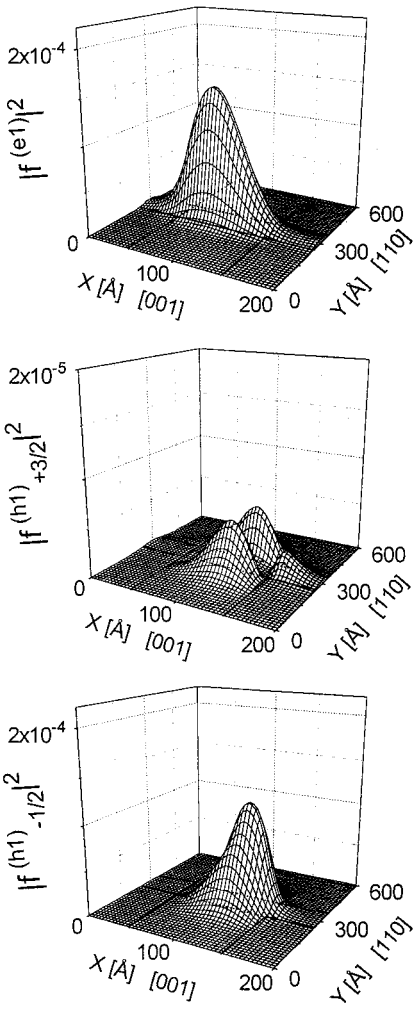

FIG. 5. Probabilities of finding in the wire the electron (upper-case drawing) and the hole with the components 3/2 and $-1/2$ (lower-case drawings), the spin quantization axis being parallel to the [110] direction of the wire. The hole potential is not sufficient to confine the hole: the hole wave function is then obtained taking into account the Coulomb attraction of the 1D confined electron.

the electrons and holes are well confined, so that it is possible to calculate the exciton binding energy R_X as usual.[20] As for the wire, it is found that the localization of electrons along the X direction always occurs in domains located on top of the CdTe layer of the SSL (so that the wire is in domain 7). For holes the localization depends strongly on the structure of the overgrown [110] CdTe/Cd_xZn_{1-x}Te QW. For a Zn concentration of 8% in the Cd_xZn_{1-x}Te, the hole is not localized in two directions: as was done for the 2D case,[21] we have to take into account the Coulomb interaction due to the 1D electron in order to confine the hole in the same wire domain as the electron one. Conversely, for a larger Zn concentration (about 20%) the hole is always localized in a different domain, namely domain 6. In the former case one obtains a spatially direct exciton (type-I-QWW), and in the latter case a spatially indirect exciton (type-II- QWW). This may explain why no QWW emission has been observed in another sample having a 24% Zn concentration for the Cd_xZn_{1-x}Te barrier of the overgrown [110] QW.

Figure 5 illustrates the calculated probabilities in the wires for the electron ground state together with the ones of the two components $+3/2$ and $-1/2$ of the hole ground state. One has to note in this figure that due to the lateral electric field along the X direction, the maxima of wave function of the electron and the hole are slightly shifted away from each other on both sides of the CdTe layer. Finally, the results of the calculation are compiled in Table I. The energy positions E and H are given with respect to those of the conduction- and valence-band edges, respectively, in bulk CdTe. It is worth noting that the QWW exciton binding energy is larger than the 2D value only if we neglect the piezoelectric effect. The latter effect, which tends to separate the electron and the hole, strongly diminishes the QWW exciton binding energy. From this calculation, an energy shift of 50 meV is found between the [110] QW and the [110] QWW (Fig. 3, arrow a) which compares very well with the 40 meV observed experimentally when exciting at low power density.

As far as the excitation density dependence is concerned, two related mechanisms are taken into account in our model. The first one is related to the increase of the band gap (blue-shift) due to the screening of electric field. The second one is related to the increase of exciton binding energy R_X (red-shift): as the result of the reduced electric field, the overlap of electron and hole wave functions is increased, which explains the difference between the calculated value of R_X with and without electric field (see Table I). Our calculation shows that the band-gap effect is dominant over the exciton binding variation effect, which is in agreement with the blue-shift observed in Fig. 3 (arrow b). However, the calculated value of the exciton energy without piezoelectric field does not account for the whole experimental energy shift. The further energy shift may come from the dissociation of the-excitons into electron-hole pairs (Fig. 3, arrow c): this ex-

TABLE I. Calculated values for the 2D [110] QW and for the [110] QWW taking into account (or not) the lateral piezoelectric field **E**. The energies E and H are given with respect to the ones of the conduction- and valence-band edges, respectively, in bulk CdTe. For the 2D [110] QW, where the electron and the hole are well confined, the exciton energy transition is given by $E_X=E_G+E+H-R_X$, with $E_G=1606$ meV. For the [110] QWW, where the hole is confined by the 1D electron, the exciton energy transition is given by $E_X=E_G+E+H$. In this case one calculates also the energy H_{2D} of the hole without including the Coulombic interaction which allows us to find a QWW exciton binding energy $R_X=H-H_{2D}$. $E_{e\text{-}h}$ is the e_1h_1 electron-hole transition energy. The energy values (a), (b), and (c) correspond to the three arrows reported at the bottom of Fig. 2.

	2D [110] QW	[110] QWW without **E**	[110] QWW with **E**
E (meV)	29	9.1	-12.4
m_e (m_0)	0.091	0.091	0.091
H (meV)	-14.1	-48.5	-33.0
m_h (m_0)	0.17	0.17 (2D)	0.17 (2D)
R_X (meV)	11.4	17	8.6
E_X (meV)	1609.5	1566.6 (b)	1560.6 (a)
$E_{e\text{-}h}$ (meV)	1620.9	1584.1 (c)	1569.2

plains the observed energy shift of the exciton recombination in the QWW. In order to explain the broadening in this high excitation regime, it should also be important to take into account many-body effects.

In summary we have studied PL spectra of $CdTe/Cd_xZn_{1-x}Te$ quantum wires that result from a modulation of the in-plane lattice constant of a quantum well grown on a $CdTe/Cd_xZn_{1-x}Te$ strained-layer superlattice. Both the large redshift of the PL line with respect to the quantum well line and its strong dependence on the excitation density can be accounted for using a model which assumes no relaxation in the sample and which takes into account the lateral piezoelectric effect present in such strain-modulated [110] wires.

We would like to thank D. Gershoni, who suggested the possibility of obtaining CdTe QWWs by strain-induced lateral confinement, and who gave us some advice concerning the optimization of the [110] growth. We are also grateful to R. Legras for technical assistance.

[1] See, for example, J. M. Gerard, in *Proceedings of the NATO Conference ''Confined Electrons and Photons: New Physics and Applications,''* edited by E. Burstein and C. Weisbuch (Plenum, New York, 1995), Vol. 340, p. 357.
[2] K. Kash, J. Lumin. **46**, 69 (1990).
[3] E. Kapon, Optoelectronics **8**, 429 (1993).
[4] R. Cingolani and R. Rinaldi, Nuovo Cimento **16**, 1 (1993).
[5] D. Gershoni, J. S. Wiener, S. N. G. Chu, G. A. Baraff, J. M. Vandenberg, L. N. Pfeiffer, K. West, R. A. Logan, and T. Tanbun-Ek, Phys. Rev. Lett. **65**, 1631 (1990).
[6] K. Kash, B. P. Van der Gaag, Derek D. Mahoney, A. S. Gozdz, L. T. Florez, J. P. Harbison, and M. D. Sturge, Phys. Rev. Lett. **67**, 1326 (1991).
[7] S. T. Chou, K. Y. Cheng, L. J. Chou, and K. C. Hsieh, J. Appl. Phys. **78**, 6270 (1995).
[8] K. Kash, D. D. Mahoney, and H. M. Cox, Phys. Rev. Lett. **66**, 1374 (1991); C. Priester (private communication).
[9] D. Gershoni *et al.*, Phys. Rev. Lett. **66**, 1375 (1991).
[10] L. Pfeiffer, K. W. West, H. L. Stormer, J. P. Eisenstein, K. W. Baldwin, D. Gershoni, and J. Spector, Appl. Phys. Lett. **56**, 1697 (1990).
[11] R. André, C. Bobin, J. Cibert, Le Si Dang, and G. Feuillet, J. Phys. (France) IV **5**, C-429 (1993); A. Dal Corso, R. Resta, and S. Baroni, Phys. Rev. B **47**, 16 252 (1993); R. André, J. Cibert, and Le Si Dang, *ibid*. **52**, 12 013 (1995).
[12] A. Ponchet, G. Lentz, H. Tuffigo, N. Magnea, H. Mariette, and P. Gentile, J. Appl. Phys. **68**, 6229 (1990).
[13] H. Mariette, F. Dal'Bo, N. Magnea, G. Lentz, and H. Tuffigo, Phys. Rev. B **38**, 12 443 (1988).
[14] C. Gourgon, Le Si Dang, and H. Mariette, J. Cryst. Growth (to be published).
[15] M. P. Halsall, J. E. Nicholls, J. J. Davies, P. J. Wright, and B. Cockayne, Surf. Sci. **228**, 41 (1990).
[16] M. Ilg, K. H. Ploog, and A. Trampert, Phys. Rev. B **50**, 17 111 (1994).
[17] G. Fishman, Phys. Rev. B **52**, 11 132 (1995).
[18] G. A. Baraff and D. Gershoni, Phys. Rev. B **43**, 4011 (1991).
[19] D. Brinkmann, A. Löffler, and G. Fishman, Nuovo Cimento (to be published).
[20] G. Bastard, *Wavemechanics Applied to Semiconductor Heterostructures* (Les Editions de Physique, Les Ulis, 1988).
[21] G. Peter, E. Deleporte, G. Bastard, J. M. Berroir, C. Delalande, B. Gil, J. M. Hong, and L. L. Chang, J. Lumin. **52**, 147 (1992).